Published in final edited form as:
Epilepsia. 2009 June ; 50(6): 1474–1483. doi:10.1111/j.1528-1167.2009.02010.x.

Subfield atrophy pattern in temporal lobe epilepsy with and without mesial sclerosis detected by high-resolution MRI at 4 Tesla: Preliminary results

Susanne G. Mueller[*], **Kenneth D. Laxer**[†], **Jerome Barakos**[†], **Ian Cheong**[*], **Paul Garcia**[‡], and **Michael W. Weiner**[*]

[*] Center for Imaging of Neurodegenerative Diseases and Department of Radiology, University of California, San Francisco, California, U.S.A.

[†] Pacific Epilepsy Program, California Pacific Medical Center, San Francisco, California, U.S.A.

[‡] Department of Neurology, University of California, San Francisco, California, U.S.A.

Summary

Purpose—High-resolution magnetic resonance imaging (MRI) at 4 Tesla depicts details of the internal structure of the hippocampus not visible at 1.5 Tesla, and so allows for in vivo parcellation of different hippocampal subfields. The aim of this study was to test if distinct subfield atrophy patterns can be detected in temporal lobe epilepsy (TLE) with mesial temporal sclerosis (TLE-MTS) and without (TLE-no) hippocampal sclerosis.

Methods—High-resolution T_2-weighted hippocampal images were acquired in 34 controls: 15 TLE-MTS and 18 TLE-no. Entorhinal cortex (ERC), subiculum (SUB), CA1, CA2, and CA3, and dentate (CA3&DG) volumes were determined using a manual parcellation scheme.

Results—TLE-MTS had significantly smaller ipsilateral CA1, CA2, CA3&DG, and total hippocampal volume than controls or TLE-no. Mean ipsilateral CA1 and CA3&DG z-scores were significantly lower than ipsilateral CA2, ERC, and SUB z-scores. There were no significant differences between the various subfield or hippocampal z-scores on either the ipsi- or the contralateral side in TLE-no. Using a z-score ≤ -2.0 to identify severe volume loss, the following atrophy patterns were found in TLE-MTS: CA1 atrophy, CA3&DG atrophy, CA1 and CA3& DG atrophy, and global hippocampal atrophy. Significant subfield atrophy was found in three TLE-no: contralateral SUB atrophy, bilateral CA3&DG atrophy, and ipsilateral ERC and SUB atrophy.

Discussion—Using a manual parcellation scheme on 4 Tesla high-resolution MRI, we found the characteristic ipsilateral CA1 and CA3&DG atrophy described in TLE-MTS. Seventeen percent of the TLE-no had subfield atrophy despite normal total hippocampal volume. These findings indicate that high-resolution MRI and subfield volumetry provide superior information compared to standard hippocampal volumetry.

Keywords

Hippocampus; Magnetic resonance imaging; Subfield; Atrophy; Temporal lobe epilepsy

Address correspondence to Susanne G. Mueller, M.D., Center for Imaging of Neurodegenerative Diseases, Department of Veterans Affairs (DVA) Medical Center, Clement Street 4150, San Francisco, CA 94121, U.S.A. susanne.mueller@ucsf.edu.

We confirm that we have read the Journal's position on issues involved in ethical publication and affirm that this report is consistent with those guidelines.

Temporal lobe epilepsy (TLE) is the most common form of partial epilepsy, with a prevalence of 0.1% in the general population (Keranen & Reikkinen, 1988). In addition to lesional TLE, which is associated with temporal mass lesions, two types of nonlesional TLE can be distinguished based on histopathologic and imaging findings: TLE with normal appearing hippocampus (TLE-no) in 30–40% of nonlesional TLE and TLE with hippocampal sclerosis/atrophy (TLE-MTS) in the remaining 60–70%. The hippocampus is not a homogeneous structure but consists of several functionally and histologically different subfields: subiculum (SUB), cornu ammonis sectors (CA) 1–3, and dentate gyrus (DG) (Duvernoy, 2005). Histopathologic studies have shown that these subfields are differently affected by different disease processes; for example, pathologic stress is associated with neuron loss in CA3, whereas Alzheimer's disease is characterized by neuron loss in CA1 (West et al., 1994; Lucassen et al., 2006). The landmark studies of Sommer (1880) and Bratz (1899) showed that hippocampal atrophy in TLE is not diffuse but is characterized by prominent neuron loss in CA1 and the DG, whereas neurons in CA2 are relatively preserved. Since then, efforts have been made to further characterize the distribution of hippocampal neuronal loss in TLE-MTS, and the following patterns have been described: (1) CA1 atrophy, (2) atrophy of the DG or end folium sclerosis, (3) atrophy of CA1 and DG, and (4) global hippocampal atrophy (Dam, 1980; Babb et al., 1984; Bruton, 1988; Wyler et al., 1992). Several studies searched for associations between different hippocampal atrophy patterns in TLE-MTS and clinical variables, and found that atrophy patterns with prominent hippocampal volume loss are more likely to be associated with good postsurgical outcome than those resulting in a small hippocampal volume loss (Mathern et al., 1995; De Lanerolle et al., 2003; Blümcke et al., 2007). These findings suggest that knowledge about extent and distribution of hippocampal neuron loss might have prognostic value in patients who are candidates for epilepsy surgery if it could be obtained before surgery.

The sensitivity of the magnetic resonance (MR) signal on a clinical 1.5 Tesla magnet is usually too low to achieve a sufficient resolution to identify individual subfields. Recent advancements with high-field magnetic resonance imaging (MRI) (3–4 Tesla) taking advantage of improved gray–white matter contrast, additional magnetization transfer effects, and T_1-weighting, allow acquisition of anatomic images at sub-millimeter resolution within a few minutes. These high-resolution images depict details of the internal structure of the hippocampus not visible at 1.5 Tesla. Using such a high-resolution protocol on a 4 Tesla MR magnet, we developed a manual marking scheme based on internal features and other hippocampal landmarks that allows the measurement of subfield specific volume losses (Mueller et al., 2007, 2008).

In this study, this technique was used with the following aims: (1) to test if this marking scheme can be successfully applied to TLE-MTS and if the typical pattern of volume loss in CA1 and/or dentate with relative sparing of CA2 described in histopathologic studies can be detected; (2) to determine if it is possible to distinguish between different patterns of hippocampal atrophy in a manner similar to that in histopathologic studies (De Lanerolle et al., 2003; Blümcke et al., 2007); and (3) to test if this technique is more sensitive for the detection of hippocampal pathology in TLE-no than the measurement of the total hippocampal volume.

Methods

Study population

The committees of human research at the University of California, San Francisco (UCSF), California Pacific Medical Center, San Francisco and VA Medical Center, San Francisco approved the study, and written informed consent was obtained from each subject according to the Declaration of Helsinki. Thirty-three consecutive patients with drug-resistant TLE were recruited between mid-2005 and the end of 2007 from the Pacific Epilepsy Program, California Pacific Medical Center, and the Northern California Comprehensive Epilepsy Center, UCSF,

where they underwent evaluation for epilepsy surgery. Fifteen patients (mean age 41.5±10.1; left TLE/right TLE 8/6, bilateral 1; females/males 10/5) had evidence (visual assessment) for mesial temporal lobe sclerosis on their 1.5 Tesla MR images (TLE-MTS) and 18 patients (mean age 37.8±8.6; left TLE/right TLE 8/10; females/males 10/8) had normal-appearing hippocampi on their 1.5 Tesla MR examinations (TLE-no); 15 of those had completely normal MR reads, one had a small cystic lesion in the left inferior temporal pole, one had an ectopic gray matter mass adjacent to the right amygdala, and one a left frontal venous angioma. Age at onset of epilepsy was different between the two groups (TLE-MTS 8.0±6.9 years; TLE-no 22.2±8.6 years; $p < 0.0001$) as was duration of epilepsy (TLE-MTS 33.2±11.4 years; TLE-no 13.5±8.7 years; $p < 0.0001$). The identification of the epileptogenic focus was based on seizure semiology and prolonged ictal and interictal video-EEG/telemetry (VET) recordings in all patients. All patients had been seizure free for at least 24 h before the MRI (cf Table 1 for patient characteristics). The control population consisted of 34 healthy volunteers (mean age 38.6±8.8; females/males 24/10).

MRI acquisition

All imaging was performed on a Bruker MedSpec 4 Tesla system controlled by a Siemens Trio console (Siemens, Iselin, NJ, U.S.A.) and equipped with a USA Instruments (Aurora, OH, U.S.A.) eight-channel array coil that consisted of a separate transmit coil enclosing the eight receiver coils. The following sequences were acquired, which were part of a larger research imaging and spectroscopy protocol: (1) For the measurement of hippocampal subfields, a high resolution T_2-weighted fast spin echo sequence (TR/TE: 3,500/19 ms, echo train length 15, 18.6 ms echo spacing, 160-degree flip angle, 100% oversampling in y direction in k space (ky) direction, 0.4 × 0.4 mm in plane resolution, 2 mm slice thickness, 24 interleaved slices without gap, acquisition time 5:30 min (adapted from Thomas et al., 2004; De Vita et al., 2003), angulated perpendicular to the long axis of the hippocampal formation; (2) For the measurement of total hippocampal volume a volumetric T_1-weighted gradient echo MRI (MPRAGE) TR/TE/TI = 2,300/3/950 ms, 7-degree flip angle, 1.0 × 1.0 × 1.0 mm^3 resolution, acquisition time 5.17 min; and (3) For the determination of the intracranial volume (ICV), a T_2-weighted turbospin echo sequence (TR/TE 8,390/70 ms, 150-degree flip angle, 0.9 × 0.9 × 3 mm nominal resolution, 54 slices, acquisition time 3.06 min).

Postprocessing and manual marking of hippocampal subfields

The method used for subfield marking including assessment of measurement reliability has been described in detail previously (Mueller et al., 2007, 2008). The marking scheme depends on anatomic landmarks, particularly on a hypointense line representing myelinated fibers in the stratum moleculare/lacunosum (Eriksson et al., 2008), which can be reliably visualized on these high-resolution images. Although the sequence used in this study provides superior resolution and thus more information about the internal structure than a clinical standard sequence, it cannot distinguish details on the resolution of a histologic preparation; therefore, we do not claim that the subfield assignment actually corresponds to the histologic subfields but merely that it provides a good approximation (cf. Fig. 1). To summarize the procedure briefly: The high-resolution images were resampled to obtain a left and a right hippocampal image on which the coronal axis was exactly perpendicular to the long axis of the hippocampus. The marking starts on the first slice on which the head of the hippocampus is no longer visible. On this slice, the hippocampal subfields [CA1-CA3, dentate gyrus (DG)], subiculum (SUB), and entorhinal cortex (ERC) are marked manually. In addition, the ERC is marked on the two slices anterior to this starting slice and the SUB and the CA1-3, including the DG, are marked on the two slices posterior to the starting slice. Altogether, hippocampal subfields were marked on five consecutive slices, that is, on a length of 1.0 cm in the rostral part of the hippocampus. The most medial point of the temporal cortex is chosen as the medial border of the ERC, and the medial end of the collateral sulcus is chosen as its lateral border. The CA1/SUB border is

determined by drawing a line perpendicular to the edge of the SUB touching the medial border of the hippocampus. This border was chosen because it could be easily and reliably identified, although by doing so parts of the presubiculum and subiculum proper were included in CA1. The CA1/CA2 border is determined by dividing the line along the longest diameter of the hippocampus by two and drawing a line perpendicular to this line. A region supposedly representing mainly CA2 was marked in a square-like manner, that is, its height at the CA1/CA2 boundary also determined its length, whereas its overall shape was determined by the course of the outer boundary of the hippocampus and the hypointense line representing myelinated tissue in the strata moleculare/lacunosum. Although the position of CA2 using the outlined criteria showed good correspondence with the localization of CA2 in histologic preparations, its volume is influenced by the width of the dorsal CA1 and it is likely to have some overlap with the dorsomedial part of CA1. Because of this overlap, we expect that volume changes in this sector can result from changes in both subfields, that is, CA2 and the dorsal part of CA1. To reflect this "contamination" by CA1, the region was named CA1-2 transition zone (CA1-2 transition) rather than CA2. The remainder of the hippocampal formation consisting of CA3 and dentate gyrus is marked as one region (CA3&DG) because there are no reliable landmarks to distinguish between these structures. The volume of the total hippocampus was determined from the T_1 image using the hippocampal masks provided by the subcortical parcellation routine of the FreeSurfer software (available at http://surfer.nmr.mgh.harvard.edu/) (Fischl et al., 2002). These hippocampal masks were visually checked for accuracy and manually edited if necessary. The ICV was calculated from the skull-stripped T_2-weighted image (BET, FMRIB Image Analysis Group, Oxford University, http://www.fmrib.ox.ac.uk/fsl/bet2/index.html was used for skull stripping).

Statistical analysis

After excluding significant side differences in controls, subfield/hippocampal volumes in this group were averaged for comparison with patients. Patient subfield/hippocampal volumes were grouped into ipsi- and contralateral volumes based on the focus lateralization as defined by VET. Multivariate analyses of covariance (MANCOVAs) with ipsilateral subfield/hippocampal volumes as dependent variables and group (TLE-MTS, TLE-no, controls), age, and ICV as independent variables were used to test for group differences and followed with multiple regression analyses and Tukey post hoc tests. A similar analysis was done for contralateral subfield/hippocampal volumes. To compare the severity of volume losses between different subfields and for individual analyses, subfield and hippocampal volumes were first normalized for head size with the following formula: normalized $\text{volume}_{\text{subject}}$ = raw $\text{volume}_{\text{subject}}$ *1,000/$\text{ICV}_{\text{subject}}$ and then converted into z-scores using the following formula: volume z-score = ($\text{volume}_{\text{subject}}$ − mean $\text{volume}_{\text{controls}}$/standard deviation $\text{volume}_{\text{controls}}$. Normalized z-scores were compared using analyses of variance (ANOVAs) and Tukey post hoc analyses. Normalized z-scores were also used to identify atrophic subfields in single subjects. For the purpose of this study, subfields with z-scores ≤ -2 were considered to be atrophied. The same criterion (z-score of total hippocampal volume ≤ -2) was used to define hippocampal atrophy.

Results

Group comparisons

The MANCOVAs revealed a significant ipsilateral group effect [group: Wilks' lambda 0.32; $F(12,114) = 7.1$; $p < 0.0001$] indicating that there are differences between TLE-MTS, TLE-no, and controls for some of the ipsilateral subfields and/or total hippocampal volumes. There were no significant group effects for contralateral subfield or hippocampal volumes; that is, contralateral subfield or total hippocampal volumes were not different between the three groups. The post hoc analyses on the ipsilateral side showed that TLE-MTS had significantly

smaller CA1, CA1-2 transition, CA3&DG, and total hippocampal volumes than controls or TLE-no. Ipsilateral subfield and total hippocampal volumes in TLE-no were not different from those in controls (cf Table 2).

To identify those subfields that are most affected in TLE-MTS, a comparison of the normalized subfield z-scores was performed using an ANOVA. A significant effect for "subfield" was found on the sclerotic side [$F(5,84) = 18.9$; $p < 0.0001$] but not on the normal-appearing side. Post hoc analyses showed that sclerotic CA1 and CA3&DG z-scores were significantly smaller than sclerotic CA2-1 transition, ERC, and SUB z-scores (cf Fig. 2A). Total hippocampal z-scores on the sclerotic side were smaller than ERC and SUB z-scores on this side. There was no significant effect for ipsi- or contralateral subfield z-scores in TLE-no. Ipsi- and contralateral ERC and CA3&DG were the subfields with the lowest z-scores in this group (−0.2 resp −0.3) (cf Fig. 2B).

Single subject analysis

For the purpose of identifying patterns of subfield atrophy in individual subjects, a z-score cut-off of ≤ -2 was chosen to identify subfields with severe volume loss. Using this approach, 14 (93%) of the 15 TLE-MTS (13 ipsilaterally, 1 contralaterally) had at least one subfield with severe volume loss, but only 11 (73%) fulfilled the criterion for total hippocampal atrophy (10 ipsilaterally, 1 contralaterally). The TLE-MTS patient who did not fulfill the criterion for severe subfield or hippocampal volume loss had a CA3&DG z-score of 1.4 on both sides (hippocampal z-scores 0.8 ipsi and 0.2 contralaterally) and evidence for bilateral independent temporal lobe epileptogenesis in the VET.

Using the threshold for severe subfield atrophy as defined earlier, the following patterns of subfield atrophy could be identified in TLE-MTS: The majority of subjects had either a global hippocampal atrophy (n = 6; atrophy of CA1, CA3&DG plus CA2, and/or SUB) or atrophy of CA1 and CA3&DG with sparing of CA1-2 transition (n = 5). A smaller group of TLE-MTS had a more restricted hippocampal volume loss, that is, two patients had predominantly CA1 atrophy and one patient predominantly CA3&DG atrophy (cf Figs. 3 and 4). TLE-MTS with extensive hippocampal volume loss, that is, global hippocampal atrophy, was not different from TLE with a more restricted volume loss (1 or 2 atrophic subfields) with respect to age at seizure onset (8.8±12.2 years vs. 7.9±3.2 years; $p > 0.05$ with Mann-Whitney test) or seizure duration (35.0±14.1 years vs. 32.3±11.6 years; $p > 0.05$ with Mann-Whitney test).

Three of 18 patients in TLE-no had evidence for a severe subfield atrophy. One TLE-no had severe ipsilateral ERC and SUB atrophy, the second bilateral CA3&DG atrophy, and the third contralateral SUB atrophy. Ipsi- and contralateral total hippocampal volumes were within the normal range in all TLE-no, including those TLE-no with isolated subfield atrophy.

Discussion

There were three major findings in this study: (1) Using a manual marking scheme based on the details of the internal structure of the hippocampus visible on a high resolution T_2-weighted image at 4 Tesla, it was possible to detect the characteristic hippocampal atrophy pattern in TLE-MTS with pronounced volume loss in ipsilateral CA1 and DG but relative sparing of CA2. (2) It was possible to identify four different atrophy patterns in TLE-MTS: The majority of TLE-MTS had either global hippocampal atrophy or atrophy of CA1 and CA3&DG. A smaller group of TLE-MTS had restricted subfield volume loss, that is, either predominantly CA1 atrophy or predominantly CA3&DG atrophy. (3) Hippocampal subfield volumetry was also able to detect ipsi- and contralateral subfield specific volume losses in 17% of TLE-no who had normal total hippocampal volumes. In contrast to TLE-MTS, volume losses were less well lateralized and found in ERC, SUB, and CA3&DG, whereas CA1 was spared, that is, the

pattern of subfield atrophy was different from those found in TLE-MTS. Taken together, these findings indicate that high-resolution hippocampal images and subfield volumetry might provide information about hippocampal pathology in TLE-MTS and TLE-no that cannot be obtained by conventional hippocampal volumetry.

The first major finding was that the increased resolution and improved signal-to-noise at 4 Tesla allowed the marking of hippocampal subfields in healthy controls and TLE patients with and without hippocampal sclerosis. The marking scheme was based on details of the internal structure of the hippocampus visible in these images. In particular, it made use of a hypointense line representing myelinated fibers in the stratum moleculare/lacunosum, which was reliably identifiable even in TLE-MTS with severe sclerosis. The preservation of the internal structure in TLE-MTS at higher field strength was not expected, since one of the main criteria for mesial hippocampal sclerosis at 1.5 Tesla in addition to the typical signal abnormality is the loss of the internal structure, which can even be found in cases without apparent hippocampal volume loss (Jackson et al., 1993, 1994). The radial distance between a point on this hypointense line and the external boundary of the hippocampus provides a good measure of the thickness of the hippocampal allocortex. However, the resolution of these images is not sufficient to identify the boundaries between different subfields, and so a set of arbitrarily defined hippocampal landmarks was used to assign different regions to different subfields. Despite this limitation, this marking scheme detected prominent volume losses in the regions assigned to CA1 and CA3&DG and significant but less severe volume losses in CA1-2 transition in TLE-MTS, which is in excellent agreement with the typical pattern of hippocampal volume loss described by histopathologic studies in this patient group (Sommer, 1880; Bratz, 1899; Dam, 1980; Wyler et al., 1992; Luby et al., 1995).

Previous studies at 1.5 Tesla used sophisticated postprocessing methods such as deformation-based or surface-based anatomic mapping techniques to identify subfield specific hippocampal volume loss in TLE-MTS (Hogan et al., 2003; Lin et al., 2005; Hogan, 2006, 2008). In contrast to our study, these studies found extensive CA1 volume losses in TLE-MTS but only mild or nonsignificant volume losses in CA3 and dentate in TLE-MTS. One explanation for the different MTS atrophy patterns found by these studies and our study is that the study populations were different; however, methodologic differences could also contribute to the different findings. Deformation-based or surface-based anatomic mapping techniques assume that subfield-specific volume losses result in an inward deformation in the region of the affected subfield and thus in a characteristic hippocampal shape change, which can be detected by a comparison of shape features between patients and controls. Although this assumption works well for processes that selectively affect “outer” hippocampal subfields (SUB, CA1, CA1-2 transition), volume losses restricted to “inner” subfields CA3 and dentate (DG and CA4)) will produce less distinctive shape changes and thus are less likely be detected by these methods particularly if they are accompanied by simultaneous changes in “outer” subfields, as this can be the case in MTS. The manual marking technique used in this study does not have these limitations, which could explain why the CA3&DG volume losses found in this study were of similar severity to those in CA1.

The second major finding was that it was possible to distinguish four different patterns of subfield volume loss in TLE-MTS: predominant CA1 atrophy, predominant CA3&DG atrophy, predominant CA1 and CA3&DG atrophy with sparing of CA1-2 transition and SUB and global hippocampal atrophy. Isolated severe volume losses in CA1 and CA3&DG were less often associated with severe total hippocampal atrophy, which explains why 93% of the TLE-MTS had regions of significant subfield atrophy but only 73% also significant total hippocampal atrophy. These patterns are in excellent agreement with the patterns described in histopathologic studies. De Lanerolle et al. (2003), for example, used neuronal cell counts and immunohistochemical methods and identified three different subgroups in a population of 151

TLE-MTS: “CA1 only” characterized by severe neuron in CA1, “MTLE/Dyn” characterized by neuron loss in CA1 and dentate and dynorphin (Dyn) negative dentate sprouting, and “MTLE” with pronounced neuronal cell loss in CA1, CA3, and dentate and massive Dyn-positive dentate sprouting. Blümcke et al. (2007) used cluster analysis to identify four different patterns of hippocampal neuronal loss in surgical specimens of 178 TLE-MTS patients: “MTS type 1a” with severe cell loss in CA1 but moderate cell loss in other subfields, “MTS type 1b” with severe cell loss in all subfields, “MTS type 2” with severe cell loss in CA1 only, and “MTS type 3” characterized by “end folium sclerosis. Patterns associated with more extensive atrophy (MTS types 1a and 1b) were more common than patterns with restricted atrophy (MTS type 2 or type 3). In both studies, patients with more pronounced hippocampal atrophy (MTLE or MTS type 1a and 1b) were more likely to become seizure free than patients with restricted neuron loss (CA1 only, MTLE/Dyn- or MTS type 3). So far, only seven TLE-MTS in this series have undergone surgery, which does not allow for a meaningful outcome assessment at the moment. However, the preliminary findings of this study suggest that subfield volumetry has not only the potential to provide more accurate information than conventional hippocampal volumetry about hippocampal atrophy in TLE-MTS, but also that this information might have predictive value for postsurgical outcome.

The third major finding was that subfield volumetry found evidence for significant hippocampal volume loss in 17% of the TLE-no, which had not been detected by conventional hippocampal volumetry. In contrast to TLE-MTS, who were characterized by—at least in this study—strictly unilateral CA1 and CA3&DG or global hippocampal volume losses (ipsilateral in 13, contralateral in 1), atrophic changes in the TLE-no subgroup were found ipsi- and contralaterally and affected CA3&DG but spared CA1. In the large majority of TLE-no patients though, ipsi- and contralateral subfield volumes were well within the normal range.

A previous study (Bernasconi et al., 2001) had found that TLE-no had significantly smaller ipsilateral ERC volumes compared to controls. Furthermore, the side with the more prominent ERC atrophy was concordant with the focus lateralization by EEG in 64% of the TLE-no. In this study, only one TLE-no had evidence for severe ERC atrophy. Although TLE-no as a group had ipsi- and contralaterally smaller ERC volumes than controls, this difference did not reach significance (ipsilateral $p = 0.18$, contralateral $p = 0.07$). The most likely explanations for the discrepancy between the two studies are on the one hand, a different and smaller study population and thus a reduced power to detect a difference in this study, and on the other hand, differences in the marking scheme used for ERC volumetry. Nonetheless, the previous study and this study both show that the pattern of hippocampal and ERC volume losses in TLE-no are clearly different from that found in TLE-MTS and thus further support the notion that that TLE-no is not just a less advanced form of TLE-MTS but more likely represents a completely different type of TLE. Further study and correlation of the two types of TLE-no (no atrophy, circumscribed atrophy) with extrahippocampal abnormalities and postsurgical outcome will be necessary to fully understand the implications of these preliminary findings.

This study has limitations: (1) The number of patients in this study is relatively small and thus the results have to be considered preliminary and need to be confirmed in a larger population. (2) Only a subset of patients ($n = 10$) has undergone surgery so far. In those patients for whom routine histopathology is available, the presence or absence of MTS has been confirmed. However, to validate the subfield-specific findings, it will be necessary to obtain subfield-specific neuronal cell counts and perform correlation analyses. This validation is currently being undertaken and will be the topic of a follow-up study. (3) The hippocampus was only marked in a relatively small region of the anterior body, and thus we might have missed atrophic changes restricted to the posterior body/tail. Although it is probably too time-consuming to mark the whole hippocampus, it is planned to mark at least a section of the posterior hippocampus in future studies because histopathologic studies have shown that patients with

atrophic changes restricted to the anterior hippocampus are more likely to benefit from surgery than patients with diffuse atrophy (Babb et al., 1984).

In conclusion, these preliminary findings suggest that high-resolution MRI at higher field strength (3–4 Tesla) depicts details of the internal structure of the hippocampal formation in TLE-MTS, which can be used for in vivo subfield volumetry. The regional selective hippocampal volume losses in CA1 and CA3&DG, with relative sparing of CA1-2 transition detected by this method, are in excellent agreement with the typical patterns of neuron loss described in histopathologic studies of TLE-MTS. In addition to this, subfield volumetry also found evidence for restricted hippocampal volume losses in about 20% of the TLE with and without MTS, which was not detected by conventional hippocampal volumetry. This indicates that subfield volumetry might be superior to conventional hippocampal volumetry for the detection of hippocampal pathologies in TLE. This information might be potentially clinically useful, since a relationship between atrophy pattern and severity and postsurgical outcome has been described in neuropathologic studies.

Acknowledgments

This work was supported by the NIH grant RO1-NS31966 to K.D.L. None of the authors has any conflict of interest to disclose.

References

Babb TL, Brown WJ, Pretorius J, Davenport C, Lieb JP, Crandall PH. Temporal lobe volumetric cell densities in temporal lobe epilepsy. Epilepsia 1984;25:729–740. [PubMed: 6510381]

Bernasconi N, Bernasconi A, Caramanos Z, Dubeau F, Richardson J, Andermann F, Arnold DL. Entorhinal cortex atrophy in epilepsy patients exhibiting normal hippocampal volumes. Neurology 2001;56:1335–1339. [PubMed: 11376184]

Blümcke I, Pauli E, Clusman H, Schramm J, Becker A, Elger C, Merschhemke M, Meenke HJ, Lehmann T, von Deimling A, Scheiwe C, Zentner J, Volk B, Romstoeck J, Stefan H, Hildebrandt M. A new clinico-pathological classification system for mesial temporal lobe sclerosis. Acta Neuropathol 2007;113:235–244. [PubMed: 17221203]

Bratz E. Ammonshornbefunde bei Epileptikern. Arch Psychiatr Nervenkr 1899;32:820–835.

Bruton, CJ. The Neuropathology of Temporal Lobe Epilepsy. Oxford University Press; Oxford: 1988.

Dam AM. Epilepsy and neuron loss in the hippocampus. Epilepsia 1980;21:617–629. [PubMed: 6777154]

De Lanerolle NC, Kim JH, Williamson A, Spencer SS, Zaveri HP, Eid T, Spencer DD. A retrospective analysis of hippocampal pathology in human temporal lobe epilepsy: evidence for distinctive patient subcategories. Epilepsia 2003;44:677–687. [PubMed: 12752467]

De Vita E, Thomas DL, Roberts S, Parkes HG, Turner R, Kinchesh P, Shmueli K, Yousry TA, Ordidge RJ. High resolution MRI of the brain at 4.7 Tesla using fast spin echo imaging. Br J Radiol 2003;76:631–637. [PubMed: 14500278]

Duvernoy, HM. The Human Hippocampus. Functional Anatomy, Vascularization and Serial Sections With MRI. Vol. 3. Springer Verlag; Berlin, Heidelberg, New York: 2005.

Eriksson SH, Thom M, Bartlett PA, Symms MR, McEvoy AW, Sisodiya SM, Duncan JS. PROPELLER MRI visualizes detailed pathology of hippocampal sclerosis. Epilepsia 2008;49:33–39. [PubMed: 17877734]

Fischl B, Salat DH, Busa E, Albert M, Dieterich M, Halsegrove C, van der Kouwe A, Killiany R, Kennedy D, Klavenes S, Montillo A, Makris N, Rosen B, Dale AM. Whole brain segmentation: automated labeling of neuroanatomical structures in the human brain. Neuron 2002;33:341–355. [PubMed: 11832223]

Hogan RE, Bucholz RD, Joshi S. Hippocampal-deformation based shape analysis in unilateral mesial temporal sclerosis. Epilepsia 2003;44:800–806. [PubMed: 12790893]

Hogan RE, Wang L, Bertrand ME, Willmore LJ, Bucholz RD, Nassif AS, Csernansky JG. Predictive value of hippocampal MR imaging high-dimensional mapping in mesial temporal epilepsy: preliminary findings. Am J Neuroradiol 2006;27:2149–2154. [PubMed: 17110686]

Hogan RE, Carne RP, Kilpatrick CJ, Cook MJ, Patel A, King L, O'Brien TJ. Hippocampal deformation mapping in MRI negative PET positive temporal lobe epilepsy. J Neurol Neurosurg Psychiatry 2008;79:636–640. [PubMed: 17928326]

Jackson DG, Berkovic SF, Duncan JS, Connelly A. Optimizing the diagnosis of hippocampal sclerosis using MR imaging. Am J Neuroradiol 1993;14:753–762. [PubMed: 8517369]

Jackson GD, Kunzniecky RI, Cascino GD. Hippocampal sclerosis without detectable hippocampal atrophy. Neurology 1994;44:42–46. [PubMed: 8290088]

Keranen T, Reikkinen P. Severe epilepsy: diagnostic and epidemiological aspects. Acta Neurol Scand 1988;78(Suppl):7–14.

Lin JJ, Salamon N, Dutton RA, Lee AD, Geaga JA, Hayashi KM, Toga AW, Engel J, Thompson PM. Three-dimensional preoperative maps of hippocampal atrophy predict surgical outcomes in temporal lobe epilepsy. Neurology 2005;65:1049–1097.

Luby M, Spencer DD, Kim JH, De Lanerolle N, McCarthy G. Hippocampal MRI volumetrics and temporal lobe substrates in medial temporal lobe epilepsy. Magn Reson Imaging 1995;13:1065–1071. [PubMed: 8750318]

Lucassen PJ, Heine VM, Muller MB, van der Beek EM, Wiegant VM, De Kloet ER, Joels M, Fuchs E, Swaab DF, Czeh B. Stress, depression and hippocampal apoptosis. CNS Neurol Disord Drug Targets 2006;5:531–546. [PubMed: 17073656]

Mathern GW, Babb TL, Vickrey BG, Melendez M, Pretorius JK. The clinical-pathogenic mechanisms of hippocampal neuron loss and surgical outcomes in temporal lobe epilepsy. Brain 1995;118:105–118. [PubMed: 7894997]

Mueller SG, Stables L, Du AT, Schuff N, Truran D, Cashdollar N, Weiner MW. Measurements of hippocampal subfields and age related changes with high resolution MRI at 4T. Neurobiol Aging 2007;28:719–726. [PubMed: 16713659]

Mueller SG, Schuff N, Raptentsetsang S, Elman J, Weiner MW. Selective Effect of Apo e4 on CA3 and dentate in normal aging and Alzheimer's disease using high resolution MRI at 4T. Neuroimage 2008;42:42–48. [PubMed: 18534867]

Sommer W. Erkrankung des Ammonshorns als aetiologisches Moment der Epilepsie. Arch Psychiatr Nervenkr 1880;10:631–675.

Thomas DL, De Vita E, Roberts S, Turner R, Yousry TA, Ordidge RJ. High resolution fast spin echo imaging of the human brain at 4.7T: Implementation and sequence characteristics. Magn Reson Med 2004;51:1254–1264. [PubMed: 15170847]

West MJ, Coleman PD, Flood DG, Troncoso JC. Differences in the pattern of hippocampal neuronal loss in normal ageing and Alzheimer's disease. Lancet 1994;344:769–772. [PubMed: 7916070]

Wyler AR, Dohan FC, Schweitzer JB, Berry AD. A grading system for mesial temporal pathology (hippocampal sclerosis) from anterior temporal lobectomy. J Epilepsy 1992;5:220–225.

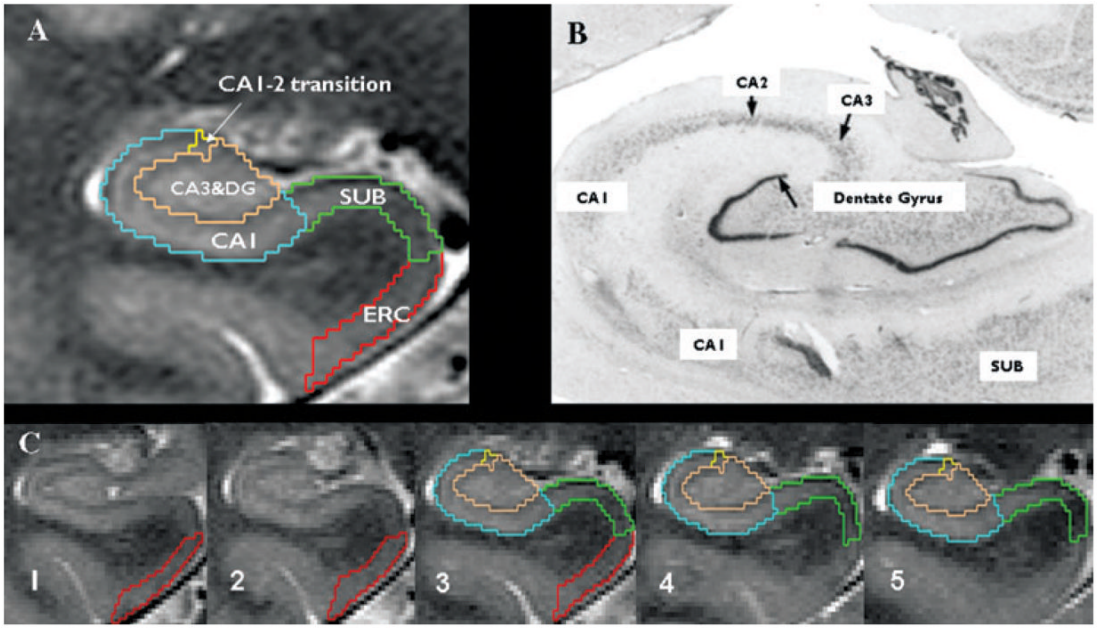

Figure 1.

(**A**) Parcellation scheme used for manual marking of subfields. Because it is not possible to identify individual hippocampal layers at 4 Tesla, the scheme was based on reliably recognizable anatomic landmarks, even though this resulted in a part of the prosubiculum or pre- and subiculum proper being counted toward the CA1 sector. ERC, entorhinal cortex; CA1-2, CA1-CA2 transition zone (cf Methods in text); CA3&DG, CA3 and dentate gyrus; SUB, subiculum. (**B**) Histologic preparation of hippocampal subfields. (**C**) Typical example of hippocampal subfield markings. No. 1 is the most anterior slice in the MRI on which subfields are marked, No. 5 the most posterior slice, and No. 3 (Slice 3), is the referred in the text as “starting” slice. Red, ERC; green subiculum; blue, CA1; yellow; CA1-2 transition; maroon, CA3&DG.

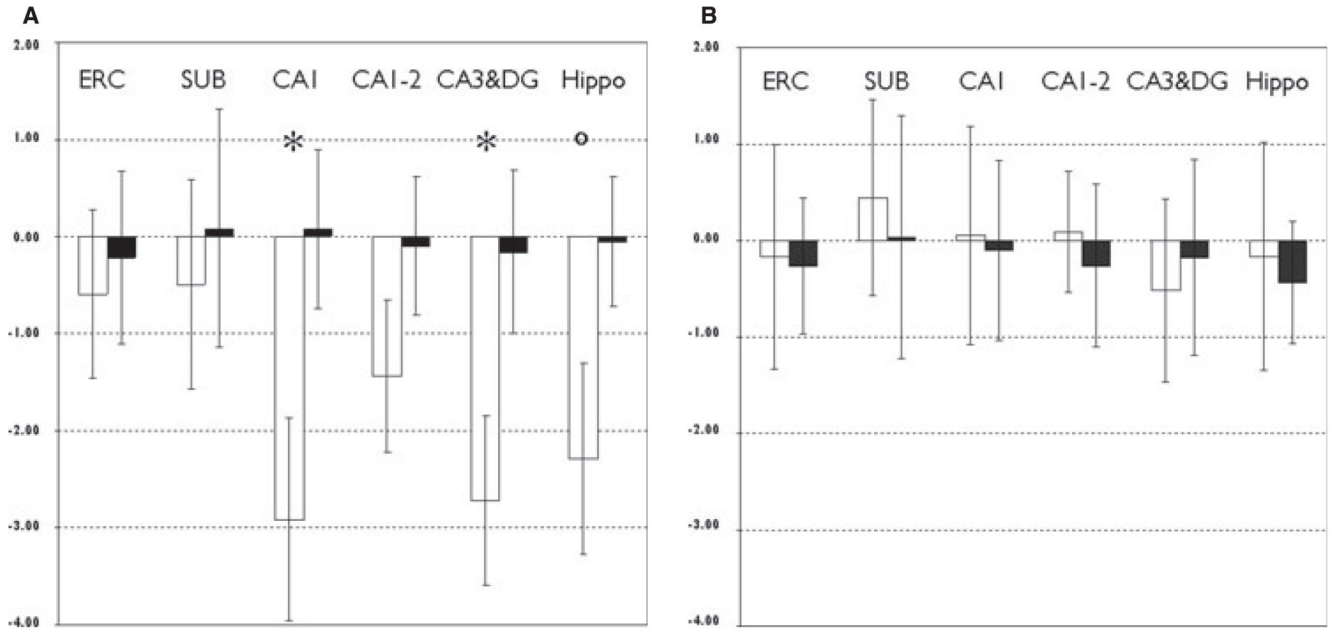

Figure 2.

Mean and standard deviation of (**A**) sclerotic and **(B**) nonsclerotic subfield z-scores in TLE-MTS (white bars) and TLE-no (black bars). *Indicates $p < 0.05$ compared to CA2. Indicates $p < 0.05$ compared to ERC and SUB. ERC, entorhinal cortex; SUB, subiculum; CA1, CA1; CA1-2, CA1-2 transition; CA3&DG, CA3 and dentate gyrus; Hippo, total hippocampal volume.

Epilepsia © ILAE

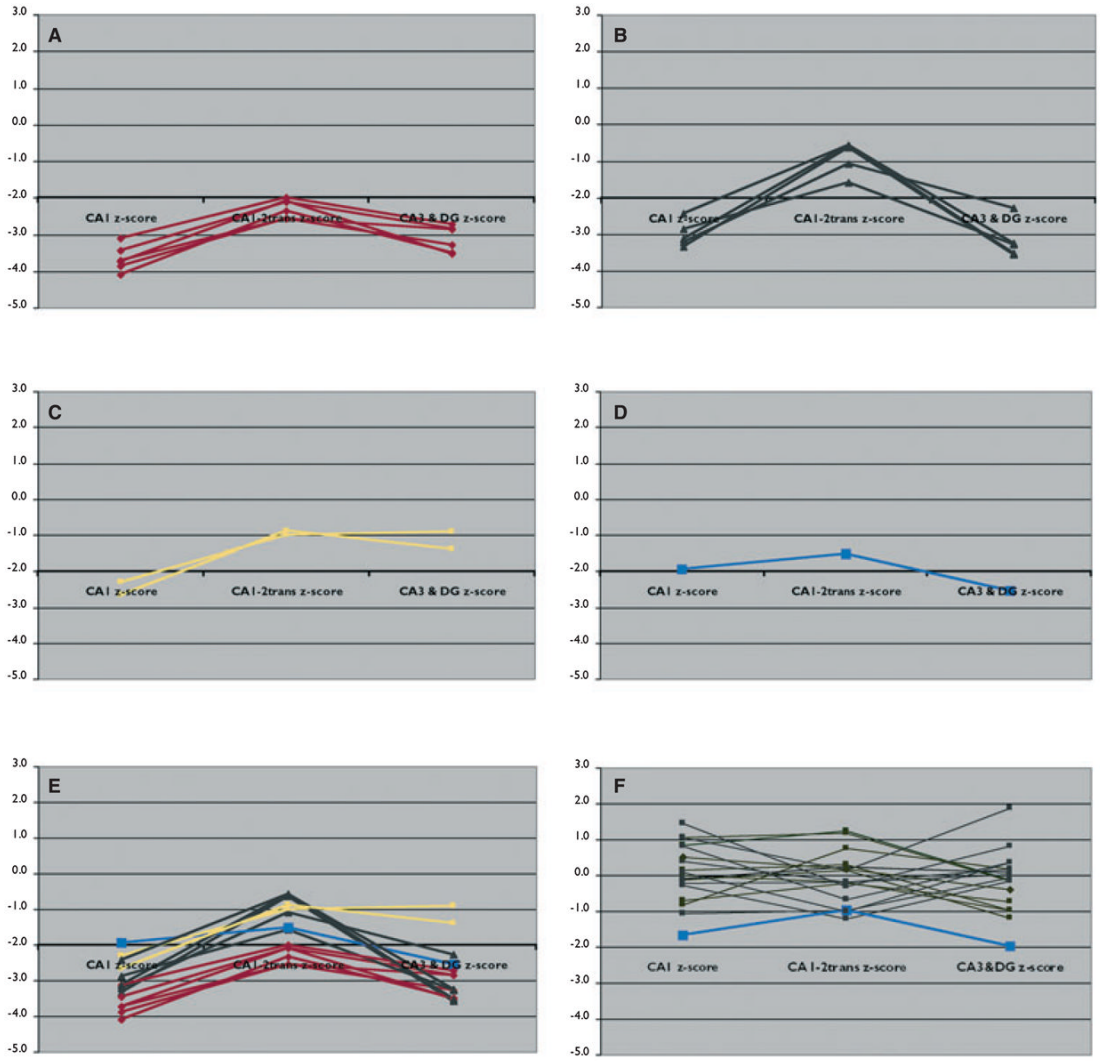

Figure 3.

Line plots demonstrating the four atrophy patterns. (**A**) Global hippocampal atrophy. (**B**) Predominantly CA1 and CA3&DG. (**C**) Predominantly CA1. (**D**) Predominantly CA3&DG. (**E**) All TLE-MTS subjects. (**F**) All TLE-no (ipsilateral), the subject indicated with the blue line fulfills the criteria for CA3&DG atrophy.

Epilepsia © ILAE

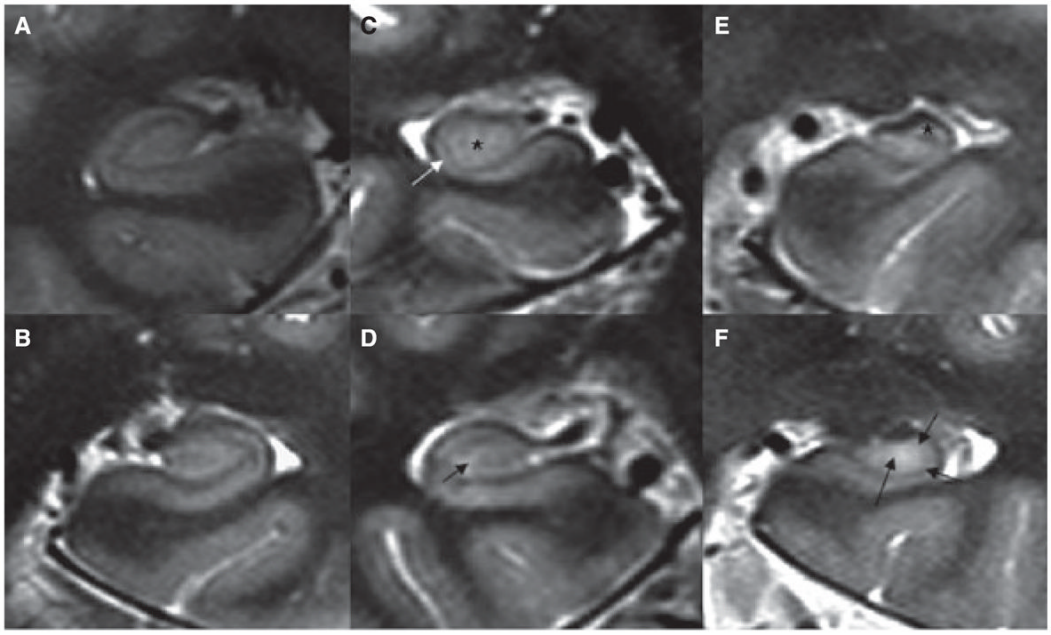

Figure 4.

High-resolution image of the hippocampus of: (**A**) 33-year-old control. (**B**) 38-year-old right TLE-no patient with normal hippocampus. (**C**) 56-year-old right TLE-MTS with isolated CA1 volume loss, the arrow indicates the relative thinning of CA1, the asterisk the normal CA3&DG. (**D**) 33-year-old right TLE-no with isolated CA3&DG volume loss; the arrow indicates the region of CA3&DG hyperintensity and volume loss. (**E**) 35-year-old left TLE-MTS with severe atrophy in CA1 and CA3&DG but relative sparing of CA1-2 transition, indicated by an asterisk. (**F**) 50-year-old left TLE-MTS with global hippocampal loss, thinning (arrows), and hyperintensity in CA1, CA1-2 transition, and CA3&DG.

Epilepsia © ILAE

Table 1

Patient characteristics

Patient No	Age	Gender	Ictal VET	Precipitating event/Risk Factors	Age at onset of seizures	1.5 Tesla clinical MRI	4 Tesla subfield MRI	Surgery/histopathology	Postsurgical outcome
1	46	Male	L mesial temporal	No	3	L MTS	L global	y/MTS	IA
2	35	Male	L mesial temporal	No	4	L MTS	L global	y/MTS	II
3	50	Female	L mesial temporal	Febrile seizures	2	L MTS	L global	y/MTS	IB
4	35	Female	L mesial temporal	No	9	L MTS	L CA1&DG	ns	
5	54	Male	L mesial temporal	No	50	L MTS	L global	ns	
6	44	Male	L mesial temporal	No	28	L MTS	L global	y/na	III
7	27	Female	Bil independent mesial temporal	Pos family history	19	L MTS	no atrophy	ns	
8	48	Female	L mesial temporal	No	13	Bil MTS	L CA1&DG	ns	
9	38	Female	L mesial temporal	Febrile seizures	6	Bil MTS	R CA1&DG	ns	
10	46	Female	R mesial temporal	Posttraumatic	6	R MTS	R CA3&DG	ns	
11	28	Female	R mesial temporal	Febrile seizures	13	R MTS	R global	y/MTS	IA
12	49	Female	R mesial temporal	No	7	R MTS	R CA1 only	y/MTS	IA
13	23	Female	R mesial temporal	Infection	5	R MTS	R CA1&DG	ns	
14	43	Male	R mesial temporal	No	5	R MTS	R CA1&DG	y/MTS	IB
15	56	Female	R mesial temporal	No	12	R MTS	R CA1 only	ns	
16	39	Male	L mesial temporal	No	29	Cystic lesion left inferior temporal pole		ns	
17	27	Female	L mesial temporal	No	10	Normal		ns	
18	33	Female	L mesial temporal	No	10	Normal		ns	
19	35	Female	L mesial temporal	No	32	Normal	R SUB	ns	
20	42	Female	L mesial temporal	No	21	Normal		ns	
21	38	Female	L mesial temporal	Posttraumatic	37	Normal		ns	
22	33	Female	L mesial temporal	No	22	Normal		ns	
23	51	Male	L mesial temporal	No	18	Normal		ns	
24	29	Male	R mesial temporal	No	11	Normal		y/normal	ID
25	43	Female	R mesial temporal	Birth complications	20	Normal		ns	

Patient No	Age	Gender	Ictal VET	Precipitating event/Risk Factors	Age at onset of seizures	1.5 Tesla clinical MRI	4 Tesla subfield MRI	Surgery/histopathology	Postsurgical outcome
26	22	Female	R mesial temporal	No	22	Left frontal venous angioma		ns	
27	45	Female	R mesial temporal	No	31	Normal	L SUB, ERC	ns	
28	33	Male	R mesial temporal	No	23	Normal	L&R CA3&DG	y/gliosis, heterotopic neurons in white matter	III
29	45	Male	R mesial temporal	Posttraumatic	30	Normal		y/normal	IA
30	30	Female	R mesial temporal	No	30	Ectopic gray matter adjacent right amygdala		ns	
31	39	Male	R mesial temporal	No	13	Normal		ns	
32	56	Male	R mesial temporal	Posttraumatic	49	Normal		ns	
33	41	Male	R mesial temporal	Posttraumatic	40	Normal		ns	

R, right; L, left; MTS, mesial temporal sclerosis; no, none; infection, meningitis or encephalitis; posttraumatic, previous head trauma but no clear temporal relationship to seizure onset; ns, no surgery; na, gamma knife, no histology; y, yes the patient had surgery; Outcome Classification; according to Engel's classification of postoperative outcome.

Table 2

Mean and (SD) of subfield and total hippocampal volumes

	Controls, n = 34	TLE-MTS, n = 15		TLE-no, n = 18	
	Mean left and right	Ipsi	Contra	Ipsi	Contra
ERC	94.6 (24.2)	78.5 (25.0)	82.8 (28.4)	88.1 (22.6)	88.4 (21.4)
Sub	89.7 (15.0)	80.8 (17.9)	93.4 (14.9)	92.7 (17.7)	90.4 (19.3)
CA1	176.7 (21.8)	104.4 (29.7)*	166.6 (35.1)	179.3 (23.2)	175.7 (23.8)
CA1-2	8.6 (1.5)	6.3 (1.2)*	8.3 (1.4)	8.4 (1.2)	8.3 (1.7)
CA3&DG	130.9 (18.5)	75.5 (22.3)*	111.3 (22.6)	129.4 (21.7)	128.3 (23.9)
Hippo	3.0 (0.5)	2.0 (0.5)*	2.7 (0.7)	3.0 (0.4)	2.8 (0.3)

Units of subfields are in cubic millimeter, unit of total hippocampus is in cubic centimeter SD.

ERC, entorhinal cortex; Sub, subiculum; CA1, CA1-2, CA1-2 transition zone; CA3&DG, CA3 and dentate gyrus; Hippo, total hippocampal volume; SD, standard deviation.

*Smaller $p < 0.05$ compared to controls.